Super-Twisting Sliding Mode Direct Torque Contol of Induction Machine Drives

Cristian Lascu
Dept. of Electrical Engineering
University Politehnica of Timisoara
300625 Timisoara, Romania
cristian.lascu@et.upt.ro

Frede Blaabjerg, Fellow IEEE
Dept. of Energy Technology
Aalborg University
9220 Aalborg, Denmark
fbl@et.aau.dk

Abstract— **This paper presents a new super-twisting sliding modes direct torque and flux controller (STSM-DTC) for induction motor (IM) drives. The STSM is a second-order (type two) variable-structure control which operates without high-frequency chattering. The proposed STSM scheme is a torque and stator flux magnitude controller implemented in the stator flux reference frame, and it does not employ current controllers as in conventional vector control. This controller contains a design parameter that allows the designer to balance its operation between a linear PI-like behavior and a constant-gain sliding-mode-like behavior. The experimental tests show that the STSM-DTC controller displays very robust behavior, similar to a conventional sliding controller, and it works without notable steady-state chattering, like the PI controller. The paper presents theoretical aspects for the new STSM-DTC control, design and implementation details, and relevant experimental results for a sensorless IM drive. The scheme is compared to a second-order sliding mode controller and a linear PI controller. A robustness assessment against the PI controller is also included.**

I. INTRODUCTION

The direct torque control (DTC) was developed as a fast and robust controller for induction machine (IM) drives in [1]. The conventional DTC employs hysteresis controllers for torque and flux, and uses the fast switching of the inverter voltage vectors to realize simultaneous control of the torque and flux magnitude. Its excellent control performance is achieved at the cost of large torque and flux ripples, which produce noise, vibrations, and losses. Recently, schemes that work with low or without torque ripple have been designed [2]-[4]. In most cases the ripple reduction was achieved by using PWM, but the robustness of the control was sacrificed.

Sliding modes control (SMC) uses fast switching of the control quantity in order to achieve a fast and robust dynamic response [5]-[6]. The closed-loop systems using SMC are stable if the external perturbations are bounded and the controller gains are large enough to compensate for the disturbance. This technique is practical in the presence of large disturbances, for systems with modeling uncertainties, or with variable parameters. During steady-state operation the SMC produces chattering of the controlled quantity. The conventional DTC is a form of SMC that takes full advantage of the voltage source inverter (VSI) switching capabilities. The VSI's voltage vectors are successively activated in order to drive the stator flux vector onto a quasi-circular path and to build up the desired torque and flux. In order to obtain a low torque ripple, very high sampling frequency must be used, which is impractical in most cases. Several practical solutions for sliding mode DTC with reduced torque and flux ripples, applied to IM drives with PWM inverters, are described in [6] and [7].

This paper investigates a DTC solution for IM drives based on the second-order super twisting sliding mode (STSM DTC) control. The STSM concept was developed in the context of the high-order SMC, which extends the first-order SMC by acting on both the higher-order time derivates of the sliding variable as well as on its first derivative. The STSM scheme uses only the control error and its integral to implement the sliding surface, it employs a nonlinear component that causes variable gains, it maintains the control robustness, and it is ripple free [8]-[12].

The paper shows that by tuning the nonlinear component is possible to balance the operation between a linear PI-like behavior and a constant-gain sliding-mode-like behavior. The paper describes the theoretical aspects of the new STSM controller, discusses the stability and gain selection criteria, illustrates the balancing between the PI and SM operation modes, and presents relevant experimental results for a sensorless IM drive. This scheme is compared with a second-order sliding mode controller from [7] and a linear PI controller described in [3]. The original contribution of this paper is the application of the STSM concept to control the torque and flux of IM drives. The experiments prove that the STSM controller has a very robust behavior, like a conventional SMC, and it works without notable steady-state chattering, like the linear PI controller. This represents a new robust and ripple-free DTC scheme for IM drives control.

978-1-4799-5776-7/14/$31.00 ©2014 IEEE

II. SUPER-TWISTING DIRECT TORQUE CONTROL

The IM model in an arbitrary reference frame (rotating at an arbitrary speed ω_e) is:

$$\underline{u}_s = R_s \underline{i}_s + \frac{\underline{\psi}_s}{\mathrm{dt}} + \mathrm{j}\omega_e \underline{\psi}_s \quad (1)$$

$$0 = R_r \underline{i}_r + \frac{\underline{\psi}_r}{\mathrm{dt}} + \mathrm{j}(\omega_e - \omega_r)\underline{\psi}_s \quad (2)$$

where $\underline{u}_s$ is the stator voltage vector, $\underline{i}_s$, $\underline{i}_r$ are the stator and rotor current vectors, $\underline{\psi}_s$, $\underline{\psi}_r$ are the stator and rotor flux vectors, ω_r is the rotor speed, R_s, R_r, are the stator and rotor resistances, and p is the number of pole pairs.

The torque Te, and the stator flux magnitude ψ_s, are:

$$T_e = 1.5p(\psi_{sd} i_{sq} - \psi_{sq} i_{sd}) \quad (3)$$

$$\psi_s = \sqrt{\psi_{sd}^2 + \psi_{sq}^2} \quad (4)$$

In the stator flux reference frame the flux is $\psi_s = \psi_{sd}$, and the torque can be obtained from (1) and (3) as:

$$T_e = \frac{3p}{2R_s}\psi_s(u_{sq} - \psi_s \omega_{\psi s}) \quad (5)$$

where $\omega_e = \omega_{\psi s}$ is the speed of the stator flux vector.

In the same reference frame the stator flux magnitude dynamics is described by (6).

$$\frac{\psi_s}{\mathrm{dt}} = u_{sd} - R_s i_{sd} \quad (6)$$

The DTC goal is to control the torque, and the stator flux magnitude. The flux is controlled by means of the direct axis voltage u_{sd}, while the torque is controlled by means of the quadrature axis voltage u_{sq}.

The STSM control is a second-order (type two) sliding mode scheme whose trajectory in the phase plane moves on a spiral (twisted) pattern while converging to the origin asymptotically or in finite time [9]-[12]. In the vicinity of the sliding surface, the control quantity converges to the equivalent control and thus the chattering can be avoided, while the other sliding mode properties and advantages are preserved. The convergence can be asymptotical or with finite time, depending on the switching scheme used. The stability can be proved for all second-order sliding mode controllers, as shown in [9].

The super twisting sliding mode flux controller is designed to change the d-axis voltage, u_{sd}, as in (7) and (8).

$$u_{sd} = K_P |s_{\psi s}|^r \mathrm{sgn}(s_{\psi s}) + u_{sd1} \quad (7)$$

$$\frac{\mathrm{d}u_{sd1}}{\mathrm{dt}} = K_I \mathrm{sgn}(s_{\psi s}) \quad (8)$$

where the flux magnitude error $s_{\psi s} = \psi_s^* - \psi_s$ is the sliding variable, and the constant gains K_P and K_I fulfill the stability criteria (see next section).

The super twisting sliding mode torque controller is designed to change the q-axis voltage, u_{sq}, as in (9) and (10).

$$u_{sq} = K_P |s_{Te}|^r \mathrm{sgn}(s_{Te}) + u_{sq1} \quad (9)$$

$$\frac{\mathrm{d}u_{sq1}}{\mathrm{dt}} = K_I \mathrm{sgn}(s_{Te}) \quad (10)$$

where the sliding variable s_{Te} is the torque error, $s_{Te} = \mathrm{T}_e^* - \mathrm{T}_e$, and the gains K_P and K_I fulfill the stability criteria.

The controllers are implemented in the stator flux reference frame. The first term in both controllers is a nonlinear discontinuous function of the sliding variable. The "amount of nonlinearity" can be controlled by changing the exponent r, which must be positive, $0 \le r \le 1$, in order to maintain the stability [9]. The second term is a function of the discontinuous time integral of the sliding variable.

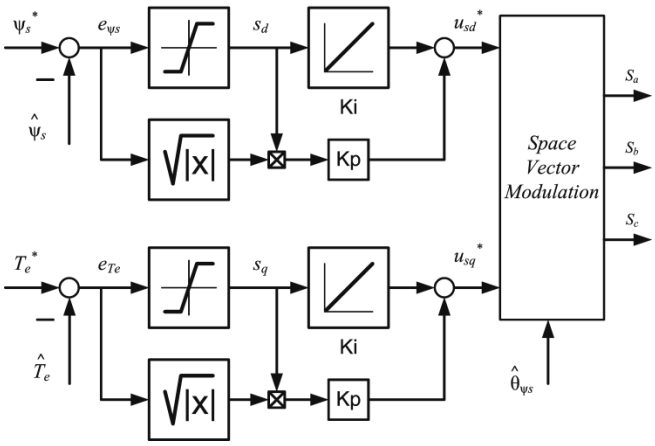

Figure 1. The STSM-DTC controller for IM drives.

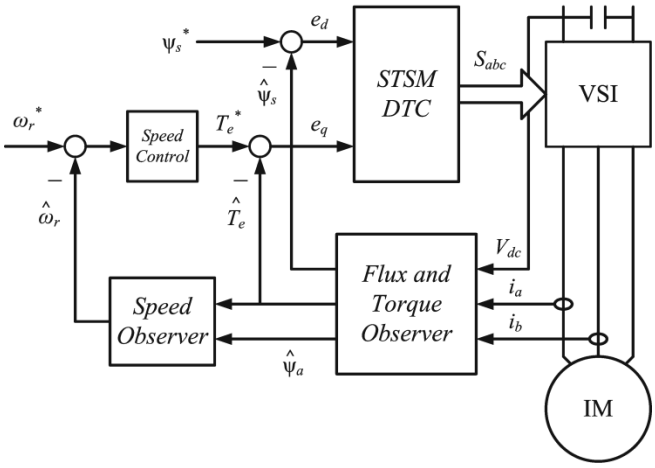

Figure 2. The sensorless IM drive with STSM DTC

The STSM DTC controller is shown in Fig. 1, and the block diagram of the sensorless IM drive which uses this controller is shown in Fig. 2. The STSM voltage output is transformed to the stationary reference frame and then the inverter PWM signals S_a, S_b, S_c are generated by means of space vector modulation (SVM). Both operations are located within the SVM block in Fig. 1.

III. Stability and Design

This section discusses the stability criteria and presents several design considerations for the STSM DTC.

A. Stability and Gain Selection

Consider a dynamic system with input u, state x and output y, described by (11).

$$\frac{\mathrm{d}x}{\mathrm{d}t} = a(x,t) + b(x,t)u, \qquad y = c(x,t) \tag{11}$$

The control problem for this system is to find a feedback control $u = f(y, \dot{y})$ that drives the system trajectories to the origin $y = \dot{y} = 0$ of the phase plane, preferably in finite time. The input u is considered a new state variable, while the switching control is applied to its time derivative, $\dot{u}$. The output y is controlled by an STSM controller, with the sliding variable $s = y^* - y$,

$$u = -K_P|s|^r \mathrm{sgn}(s) + u_1 \tag{12}$$

$$\frac{\mathrm{d}u_1}{\mathrm{d}t} = -K_I \mathrm{sgn}(s) \tag{13}$$

This controller does not use the derivative of the sliding variable. The sufficient condition for convergence to the sliding surface and for stability is for the gains to be large enough, as imposed by (14) [9].

$$K_P > \frac{A_M}{B_m}, \qquad K_I \geq \frac{4A_M}{{B_m}^2} \cdot \frac{B_M(K_P + A_M)}{B_m(K_P - A_M)} \tag{14}$$

where $A_M \geq |A|$ and $B_M \geq B \geq B_m$ are upper and lower bounds of A and B in the second derivative of y.

$$\frac{\mathrm{d}^2 y}{\mathrm{d}t^2} = A(x,t) + B(x,t)\frac{du}{dt} \tag{15}$$

For the torque and flux controllers the second derivatives of the outputs are calculated from (3) and (6). The second derivative of the flux magnitude is:

$$\frac{\mathrm{d}^2 \psi_s}{\mathrm{d}t^2} = -R_s \frac{\mathrm{d}i_{sd}}{\mathrm{d}t} + \frac{du_{sd}}{dt} \tag{16}$$

which gives $A = -R_s \mathrm{d}i_{sd}/\mathrm{d}t$ and $B = 1$. The stator current derivative in the stator flux reference frame is:

$$\frac{\mathrm{d}\underline{i_s}}{\mathrm{d}t} = -a\underline{i_s} + \frac{1}{L_s\sigma} b\underline{\psi_s} + \frac{1}{L_s\sigma}\underline{u_s} \tag{17}$$

where $a = \frac{1}{T_s\sigma} + \frac{1}{T_r\sigma} + \mathrm{j}(\omega_{\psi s} - \omega_r)$, $b = \frac{1}{T_r} - \mathrm{j}\omega_r$, T_s and T_r are the stator and rotor time constants, L_s and L_r are the stator and rotor inductances, L_m is the magnetizing inductance, and $\sigma = (L_s L_r - L_m^2)/L_s L_r$.

The current, flux, voltage, and speed are all bounded, which makes the current first derivative bounded. Therefore the first term in (16) is bounded and the K_P gain must be larger than that value.

Assuming constant stator flux magnitude and constant or slowly variable speed, the second derivative of the torque is calculated from (3) and (17):

$$\frac{\mathrm{d}^2 T_e}{\mathrm{d}t^2} = 1.5p\psi_s \left(\mathcal{R}e(-a\frac{\mathrm{d}\underline{i_s}}{\mathrm{d}t}) + \frac{1}{L_s\sigma}\frac{du_{sd}}{dt}\right) \tag{18}$$

Thus $A = 1.5p\psi_s \mathcal{R}\mathrm{e}(-a\mathrm{d}\underline{i_s}/\mathrm{d}t)$ and $B = 1.5p\psi_s/L_s\sigma$, which are both bounded due to the same reasons as before. Therefore, both gains can be selected according to (14).

The assumption of constant or slowly variable speed and flux is practical for most situations. The flux is kept constant by the flux controller, or changes slowly with the speed during field weakening. Due to mechanical inertia the speed dynamics is at least one order of magnitude slower than the current and torque dynamics.

Overall, changing the K_P gain is the most effective way to control the response time for both torque and flux, while the K_I gain influences the steady state control accuracy. A too large value for K_P has a negative impact on the torque ripple during steady state operation. The suggested gain selection procedure is as follows.

Step 1: with $r = 0$, or some r_{min} value, select K_P for the desired response time, ignoring the chattering for now. For example, for the torque response tests in Fig. 11, $K_P = 40$ was set for a 2.5 ms response time, at $r = 0$, while for Fig. 5, $K_P = 100$ was set for a 2 ms response time. For the flux controller, the flux rising time has a strong impact on the startup peak current. In this case K_P must be low enough to keep the peak current below the trip limit.

Step 2: with $r = 1$, or some r_{max} value, select K_I for the desired overshoot and settling time. For the flux response tests in Fig. 12, $K_I = 2000$ was set to keep the overshoot below 10% of the rated flux. For the torque controller the goal was to work without visible overshoot and a smooth settling, as in Fig. 6.

Step 3: increase r until the torque and flux ripples vanish, with an eye on the flux response time which also changes. Values in the range $r = 0.1$ to 0.5 are practical for low power drives. See next section for a discussion on r.

The following constant gains have been used for all experiments which are described in the following sections: for the flux controller: $K_P = 200$, $K_I = 2000$, $r = 0.1$; torque controller $K_P = 100$ or 40, $K_I = 2000$, $r = 0.4$, which are well above the limits imposed by (14).

B. Controller Behavior Selection

Both controllers employ a nonlinear quantity, the control error magnitude at power r which multiplies the proportional gain K_P. In this way K_P becomes adaptive with the error magnitude. Changing the exponent r modifies the controller behavior in a substantial way. Consider the proportional component in (7) and (9): $K_P|s|^r\text{sgn}(s)$, where s stands for any of the two sliding variables. With r = 1 this term becomes continuous and proportional with the error ($K_P|s|\text{sgn}(s) = K_P s$), and (7) and (9) turn into asymptotical PI controllers with constant gains. With r = 0 the first term becomes discontinuous $K_P\text{sgn}(s)$, which denotes a constant-gain sliding mode controller (SMC) [7]. Both cases have been tested in our experiments. The block diagram for direct torque and flux SMC is shown in Fig. 3. The SMC is known as being very robust and has finite time convergence.

A convenient way to find a balance between these two situations is to use fractionary values for r. In this case the control remains a sliding mode one, and this parameter has the effect of modifying the apparent sliding mode P gain (i.e. the aggregated gain $K_P|s|^r$) when the control error changes. When the control error is larger than 1 the controller output is reduced, while for errors smaller than 1 the output will be increased, both with respect to the output of a linear proportional controller. This sliding mode effect is stronger as r approaches zero, i.e. the apparent gain changes less and remains relatively large for small errors. In this case the controller behaves like a sliding controller and the chattering increases. On the other hand, when r moves towards 1, the apparent gain changes with s, and the controller operation approaches that of a linear PI controller, whose output changes in proportion with the control error. The chattering vanishes, but overshooting may occur more frequently. When the error is zero the apparent sliding gain is always zero, which allows the sliding mode operation with reduced chattering, even when r is relatively small. Figure 4 shows the normalized (K_P = 1) transfer characteristic of the proportional component for r = 0, 0.3 and 1. As r changes the green curve bends between the red and blue lines. The integral component of both controllers is always smooth and it becomes dominant as the error approaches zero. In the same time, the proportional component becomes small and thus the steady state operation is without chattering.

For both controllers, several values have been tested for r, for a 0.5 kW and a 1.1 kW IM drive, and the results are presented in the next section. The conclusion is that the most practical values are $r \le 0.5$, with values in the range 0.4-0.5 for torque and 0.1-0.2 for flux. In this way, both controllers operate like robust sliding controllers with very low chattering (practically no visible ripples). In general, the flux shows very low ripples due to the large time constants, and the flux controller can be pushed more aggressively towards the sliding mode operation, with benefits in control robustness. The torque controller is quite sensitive to noise and a very narrow saturation band of 0.02 Nm has been used to reduce the ripples when r is less than 0.4.

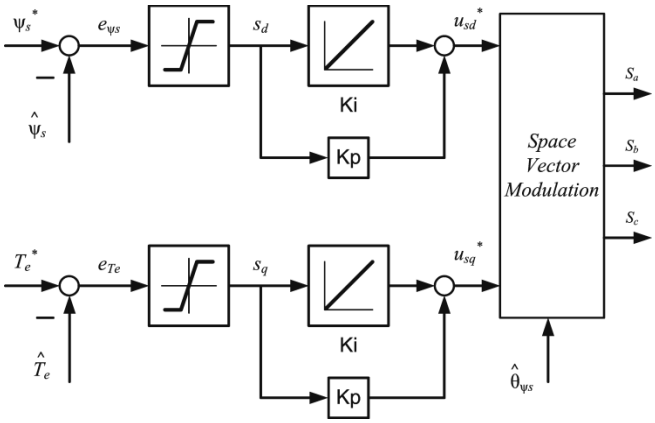

Figure 3. The sliding-mode direct torque and flux controller (r = 0).

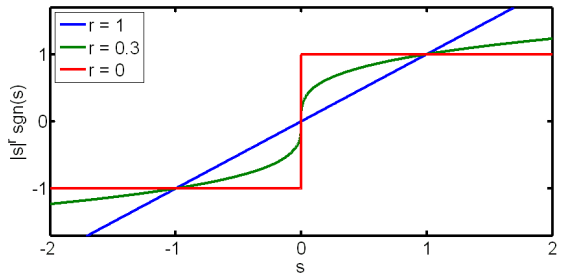

Figure 4. Transfer characteristic of the P component for r = 0, 0.3, 1.

IV. Experimental Results and Comparison

The STSM DTC was tested on two IM drives. The results presented in this section are for the 0.5 kW IM drive with nameplate data: U_N = 400 V, I_N = 1.5 A, f_N = 50 Hz, T_N = 3 Nm, p = 2. Te motor parameters are: R_s = 16 Ω, R_r = 18.5 Ω, L_s = L_r = 0.769 H, L_m = 0.722 H. The voltage source inverter is a 2.2 kVA FC302 inverter with open control, from Danfoss Drives. The control system is implemented in C++ on a TMS320F28335 DSP from Texas Instruments. The sampling and switching frequencies are f_s = 10 kHz. Two currents and the dc link voltage, V_{dc}, are measured. The actual stator voltage is calculated from the switching signals and V_{dc}. The torque, flux, and speed shown in this section are estimated by a full-order state observer described in [14].

A. Dynamic Response

The torque and flux dynamic response was tested with the following scenario: from standstill, at t = 65 ms, the flux reference was set to ψ_s^* = 0.95 Wb, and the torque reference was set T_e^* = 4 Nm (130 % rated torque) at t = 100 ms, both steps. Fig. 5 shows the torque and flux control performance of the STSM controller. The gains used for this test are: flux controller: K_P = 200, K_I = 2000, r = 0.1; torque controller K_P = 100, K_I = 2000, r = 0.4. The torque reaches the set point in 2 ms, while the flux needs 35 ms, both without overshoot. Doubling K_P will decrease the set time to below 1 ms. These time values are comparable to those for a standard DTC. During this test the rotor speed remains low.

During transients the waveforms show typical sliding mode behavior with almost constant slope. During steady state operation both are without notable ripple, like linear controllers. Similar results have been obtained for the 1.1 kW drive, with the same controller gains.

For comparison, Fig. 6 shows the torque and flux control performance of the Linear DTC controller. This was operated with the same K_P and K_I gains as the STSM.

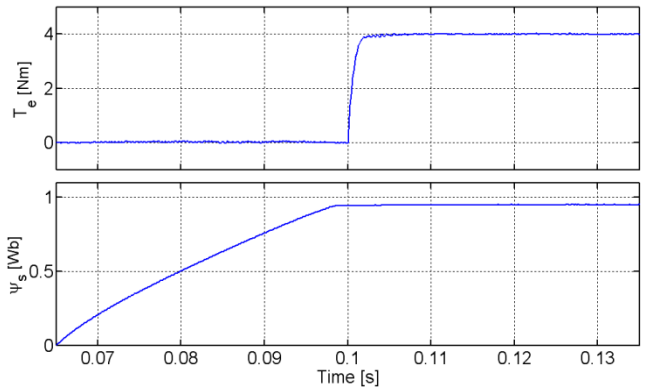

Figure 5. Torque and flux dynamic response with STSM-DTC (r = 0.4).

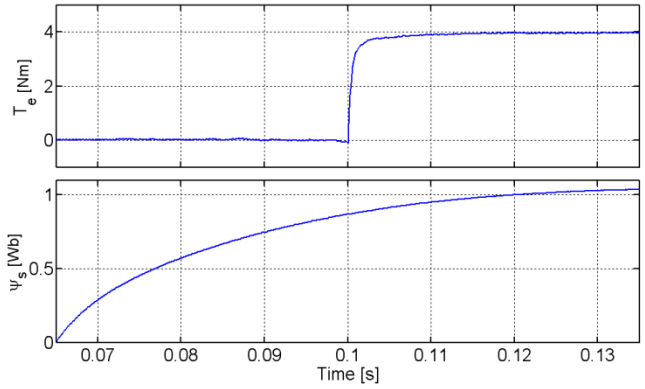

Figure 6. Torque and flux dynamic response with Linear DTC.

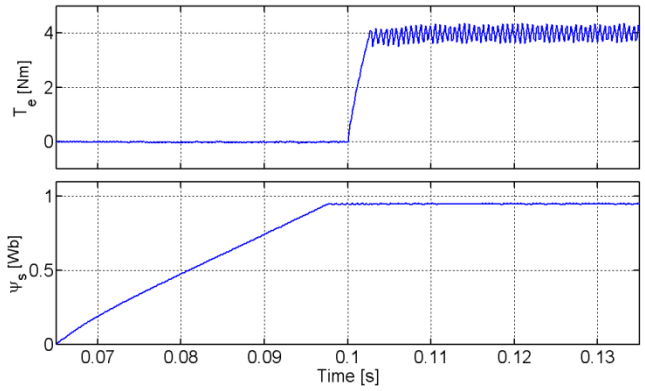

Figure 7. Torque and flux dynamic response with SMC (r = 0).

The Linear DTC uses PI controllers in the stator flux reference frame, for torque and flux [3]:

$$u_{sd} = \left(K_P + K_I \frac{1}{s}\right) s_{\psi s} \tag{19}$$

$$u_{sq} = \left(K_P + K_I \frac{1}{s}\right) s_{Te} \tag{20}$$

The torque response is comparable to that for STSM, with longer settling time, but the flux needs a much longer time to reach the reference and has overshoot.

The STSM-DTC was also compared with a sliding mode controller SMC, shown in Fig. 3, obtained with r = 0 for both controllers. The torque and flux response is shown in Fig. 7, where the torque chattering is visible. Thus, the most important advantage of STSM over SMC is the absence of torque chattering during steady state operation. Both controllers are robust as demonstrated next.

B. Control Robustness

The robustness of a sensorless drive is mostly determined by the robustness of its state observer. The observer used for this drive is reasonably accurate and its analysis is beyond the scope of this paper [14]. Here we only investigate the *control robustness* of STSM DTC with respect to Linear DTC, with the observer and all other implementation details being the same. The controller gains do not depend on the motor parameters and parameter detuning has no effect on the controller operation. However, due to some estimation errors the field orientation may be imperfect, and the drive exhibits a small amount of cross-coupling effect between the d and q axes.

Fig. 8 shows the STSM DTC performance (from top to bottom: speed, torque, and flux magnitude, all estimated) during large speed and torque transients – fast reversals at rated speed. Fig. 9 shows the same quantities during a similar test with Linear DTC. Both controllers use the same gains as for Figs. 5 and 6. Notably the STSM flux controller is very robust to speed and torque transients – the flux is constant, unlike the Linear DTC which shows flux oscillations of about ±5% during the reversals. The torque is also very well controlled at 4 Nm in the case of STSM, while the Linear DTC shows some torque oscillations. This denotes that the torque controller is robust with respect to perturbations. The torque oscillations at constant speed are due to the variable load torque – a PMSM with large cogging torque is mechanically connected to the IM. The SMC controller (r = 0), not shown, behaves similarly to the STSM, only with larger torque ripple.

C. Low speed Operation

The low speed performance is illustrated in Fig. 10 which shows the torque and flux control during torque reversals at low speeds. For this experiment the speed reference reverses each 250 ms, and the PI speed controller produces a square torque reference. Furthermore, the torque rate of change was limited to 200 Nm/s.

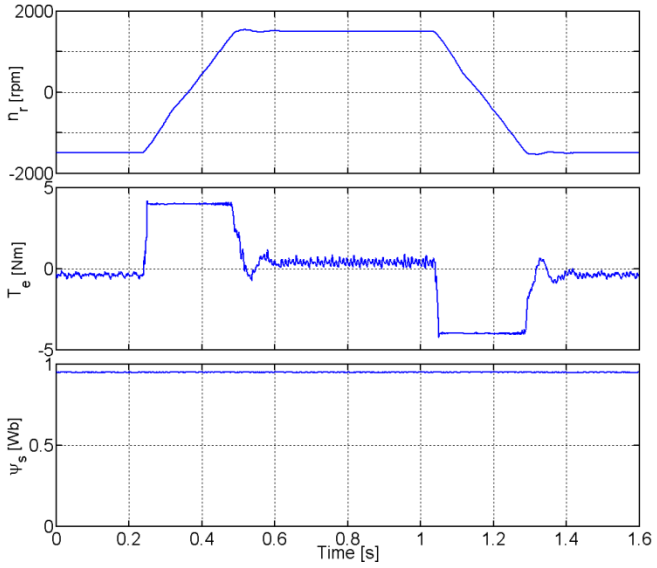

Figure 8. Speed and torque transients with STSM-DTC; from top to bottom: speed, torque, and flux magnitude.

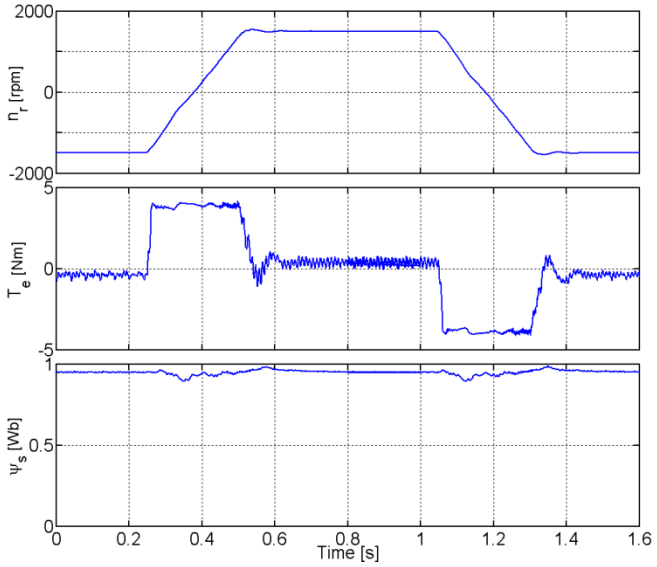

Figure 9. Speed and torque transients with Linear DTC; from top to bottom: speed, torque, and flux magnitude..

In this way, the drive runs at variable low speed with a trapezoidal torque reference. The estimated torque is the top trace in Fig. 10, and this test illustrates the excellent tracking performance of the STSM controller – the torque completely overlaps its reference. The bottom graph shows the estimated stator flux (blue) and rotor flux (red) magnitudes. As for the high speed operation, the torque and flux ripples are absent and the drive is robust, with the stator flux very well controlled. Faster slopes for the torque reference produce identical results. The same gains as for the previous test have been used.

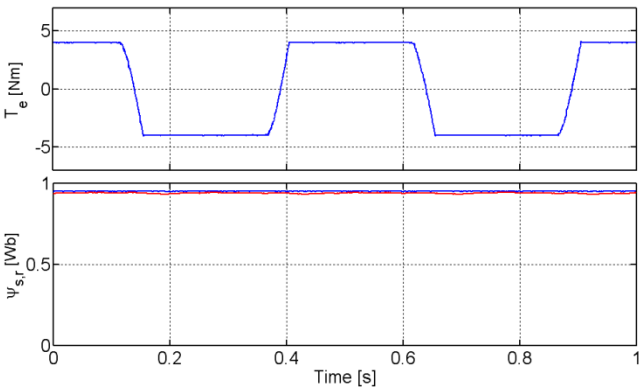

Figure 10. Torque reversals at low speed with STSM; top: torque; bottom: rotor flux - red, stator flux - blue.

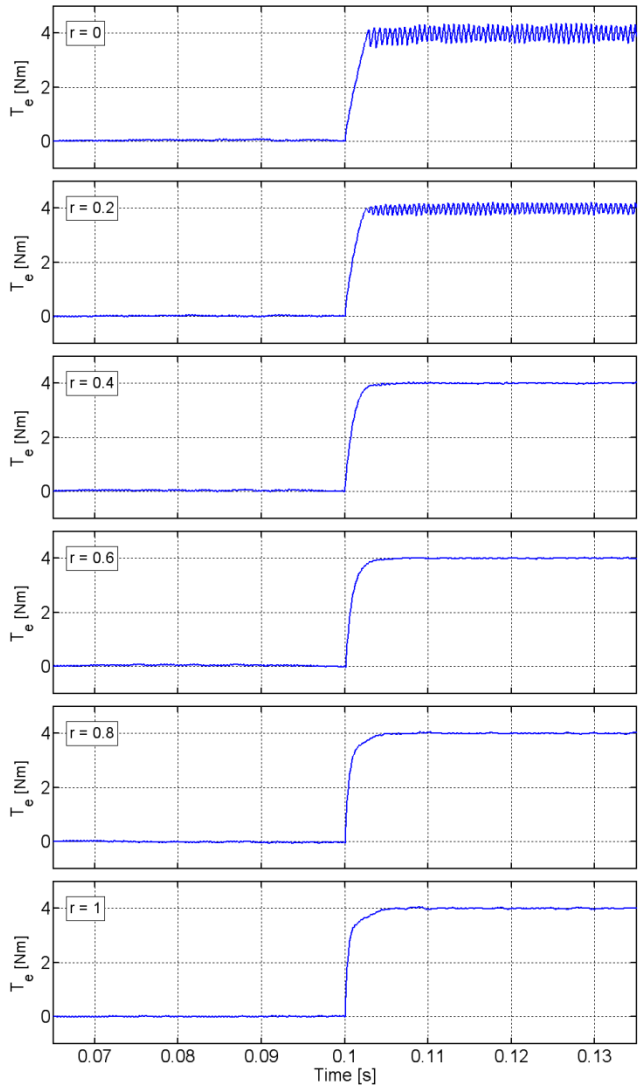

Figure 11. STSM-DTC torque response with $r = 0$ to 1.

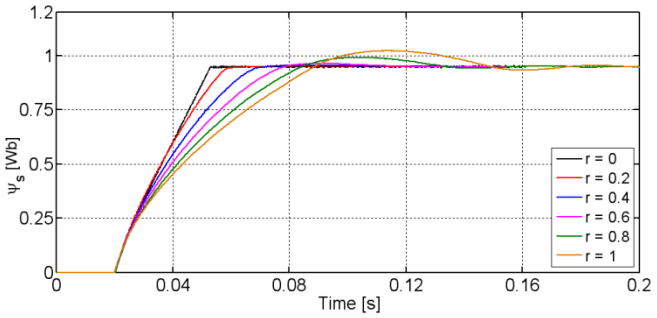

Figure 12. STSM DTC flux response with r = 0 to 1.

D. Controller Gain Selection

This section investigates the STSM controller balancing between SMC and quasi-linear operation when the parameter r is modified. The effect of changing r for the torque controller is illustrated in Fig. 11, which shows the torque response for r = 0 to 1. Sliding mode typical behavior and chattering occur for values less than 0.4, while settling time is longer for values close to 1. The other PI gains are: K_P = 40, K_I = 2000, for a response time of 2.5 ms at r = 0.

The flux response is shown in Fig. 12 for r = 0 to 1. The typical SMC operation and some low ripple are apparent for low values of r, while PI-like overshoots occur for large values. Notice the impact of changing r on the response time. The values around 0.1-0.2 are preferred for a fast response with low chattering. It is notable that parameter r has a substantial impact on the steady state and transient operation. For a real drive, when more flexibility is desired. the controller may benefit from real time adaptation of parameter r, especially when the control errors are large.

V. Conclusion

This paper proposes a super twisting sliding mode controller for torque and flux control in induction machine drives. This is a new DTC scheme for sensorless IM drives and it has the following salient features.

STSM is very robust with respect to speed and torque transients, to load perturbations, and to observer inaccuracy. The experiments show that the STSM preserves the excellent robustness of the sliding mode control at all speeds. This is a major advantage over the Linear DTC.

The second advantage is that the STSM operates without visible chattering, acoustic noise or vibrations. In this respect it is similar to the Linear DTC. The dynamic operation is as fast and precise as that of a conventional DTC. During transients STSM displays typical sliding modes behavior, while during stationary operation behaves almost like a linear controller. By tuning the parameter r for the nonlinear component it is possible to balance the operation between a linear PI-like behavior and a constant-gain sliding-mode-like behavior.

This controller offers a convenient, simple way to tune the response time by changing K_P, unlike the conventional DTC, whose response time is fast but not tunable.

Overall, the new STSM controller combines the main advantages of the sliding mode control, linear PI control, and conventional DTC. The paper describes the theoretical aspects of the STSM-DTC, discusses the stability and gain selection criteria, illustrates the balancing between the PI and SM operation modes, and presents relevant experimental results for a low power sensorless IM drive.

References

[1] I. Takahashi, T. Noguchi, "A New Quick Response and High Efficiency Control Strategy of an Induction Motor," Rec. IEEE IAS, 1985 Annual Meeting, pp. 495-502, 1995.

[2] D. Casadei, G. Serra, A. Tani, "Implementation of a direct torque control algorithm for induction motors based on discrete space vector modulation," IEEE Trans. Power Electronics, vol. 15, no. 4, July 2000, pp. 769-777.

[3] C. Lascu, I. Boldea, F. Blaabjerg, "A modified direct torque control for induction motor sensorless drive," IEEE Trans. Industry Applic., vol. 36, no. 1, Jan./Feb. 2000, pp. 122-130.

[4] Y.-S. Lai, W.-K. Wang, Y-C. Chen, "Novel switching techniques for reducing the speed ripple of ac drives with direct torque control," IEEE Trans. Industrial Electronics, vol. 51, no. 4, Aug. 2004, pp. 768-775.

[5] V. Utkin, J. Guldner, J. Shi, Sliding Mode Control in Electromechanical Systems, Taylor & Francis, 1999.

[6] Z. Yan, C. Jin, V.I. Utkin, "Sensorless sliding-mode control of induction motors," IEEE Trans. Industrial Electronics, vol. 47, no. 6, Dec. 2000, pp. 1286-1297.

[7] C. Lascu, I. Boldea, F. Blaabjerg, "Variable-structure direct torque control – A class of fast and robust controllers for induction machine drives," IEEE Trans. Industrial Electronics, vol. 51, no. 4, Aug. 2004, pp. 785-792.

[8] A. Levant, "Sliding order and sliding accuracy in sliding mode control", Int. Journal of Control, vol. 58, no. 6, June 1993, pp. 1247-1263.

[9] A. Levant, "Higher-order sliding modes, differentiation and output-feedback control", Int. Journal of Control, vol. 76, no. 9, Sept. 2003, pp. 924-941.

[10] A. Levant, "Principles of 2-sliding mode design", Automatica, vol. 43, no. 4, Apr. 2007, pp. 576-586.

[11] A. Levant, "Quasi-continuous higher-order sliding-mode controllers", IEEE Trans. Autom. Control, vol. 50, no. 11, Nov. 2005, pp. 1812-1816.

[12] S. DiGenaro, J. Rivera, B. Castillo-Toledo, "Super-twisting sensorless control of permanent magnet synchronous motors", IEEE Conf. on Decision and Control, Dec. 2010, pp. 4018-4023.

[13] T. Gonzales, J.A. Moreno, L.Fridman, "Variable gain super twisting sliding mode control", IEEE Trans. Automatic Control, vol. 57, no. 8, Aug. 2012, pp. 2100-2105.

[14] S. Jafarzadeh, C. Lascu, S.M. Fadali, "Square root unscented Kalman filters for state estimation of induction motor drives", IEEE Trans. Industry Applications, vol. 49, no. 1, Jan.-Feb. 2013, pp. 92-99.